



# Large scale structures in the Universe: a multi-frequency (re)view

S. Colafrancesco

ASI - ASDC, Via G.Galilei snc, I-00040 Frascati (Roma), Italy  
Email: sergio.colafrancesco@asi.it

**Abstract.** We discuss a physical description of large scale structures in the universe that takes into account many relevant aspects of structure formation and evolution: Dark Matter, baryonic gas, cosmic rays, magnetic fields and Black Holes. After discussing a few specific example of such multi-disciplinary study of LSS, we delineate an experimental outline aimed to link the multi-disciplinary approach with the multi-frequency study of LSS in the universe.

## 1. Introduction

Large Scale Structures (LSS) in the universe are the repositories of the traces, of the history and of the composition of cosmic structures. Galaxy clusters, the largest gravitationally bound structures in the universe, are the representative systems of the distribution of LSS in the universe.

The description of these cosmic structures is continuously enriching of physical details regarding their matter and field content.

**Dark Matter** (DM) is the dominant form of matter that creates the potential wells of cosmic structures, from those on the largest scales down to galactic and sub-galactic scales (see Fig.1). If we consistently take into account the fundamental nature of DM particles,<sup>1</sup> we are inevitably bound to consider the effects of

their annihilation (in the case of SUSY DM particles) or their decay (in the case of sterile neutrinos) on the structure and evolution of the DM clumps (see Colafrancesco 2009a for a review, see Fig.1).

**Baryonic material** collected in the DM potential wells of LSS is likely heated and shocked by large-scale shock waves found in cosmological simulations (see, e.g. Ryu et al. 2003, Pfrommer et al. 2006) which produce a complex distribution of Mach numbers, with shock velocities  $V_{shock} \lesssim 250$  km/s at the intergalactic shocks and  $250 \lesssim V_{shock} \lesssim 1000$  km/s at shocks found inside clusters (see, e.g. Ryu et al. 2003). LSS shock waves have been suggested to exist in large scale filaments (see Bagchi et al. 2002 for the case of the large-scale filament ZwCl 2341.1+0000) and in clusters (see Sarazin 2001 for a review). The presence of shock waves with relatively high Mach numbers naively suggest that Fermi-like acceleration might take place in LSS thereby accelerating **cosmic rays** (CRs) that can be efficiently confined mainly in galaxy clusters (see e.g. Colafrancesco &

---

*Send offprint requests to:* S. Colafrancesco

<sup>1</sup> Viable candidates for the DM are neutralinos (the lightest MSSM particles, see Jungman et al. 1996), sterile neutrinos (the lightest right-handed neutrino, see Shaposhnikov 2007) or even other forms of light DM, see Boyanovsky et al. 2007).

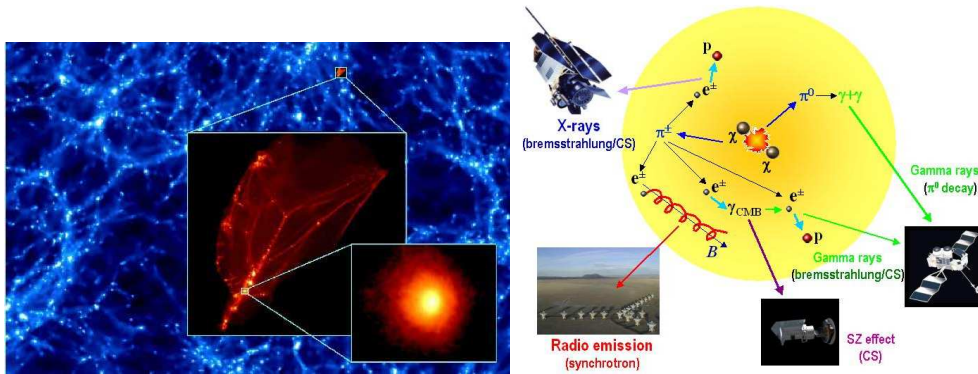


**Fig. 1.** Left. A simulation of DM distribution in LSS. The zoom-up insets show the DM distribution in progressively small-scale structures (courtesy of J. Diemand). Right. A simple model which shows the basic astrophysical mechanisms underlying the search for the nature of DM particles ( $\chi$ ) through the emission features occurring in large-scale structures. These mechanisms are, among others:  $\gamma$ -ray emission from  $\pi^0 \rightarrow \gamma + \gamma$ , relativistic bremsstrahlung of secondary  $e^\pm$  and ICS of CMB photons by secondary  $e^\pm$ ; X-ray/UV emission due to non-thermal bremsstrahlung and ICS of background photons by secondary  $e^\pm$ ; synchrotron emission by secondary  $e^\pm$  diffusing in the intra-cluster magnetic field;  $SZ_{DM}$  (ICS of CMB photons by secondary  $e^\pm$ ) effect.

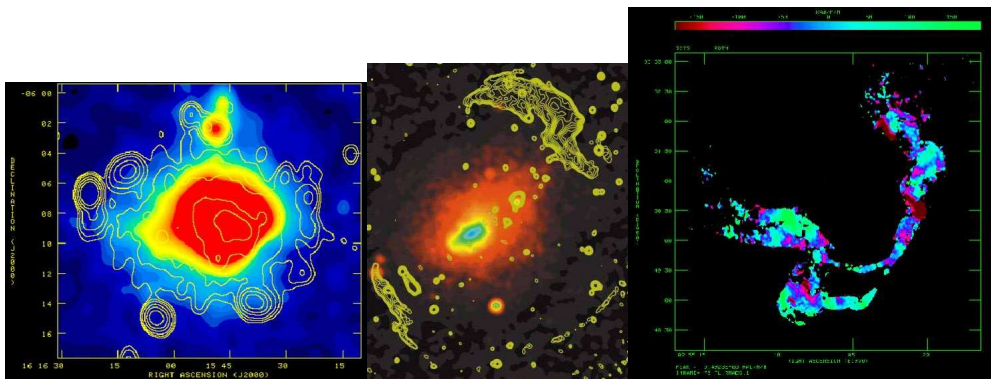


**Fig. 2.** Left. A composite radio (colors) and X-ray (contours) image of the giant radio-halo cluster A2163. Middle. A composite radio (contours) and X-ray (colors) image of the cluster A3667 that contains two symmetric radio relics. Right. A Faraday Rotation image of the radio lobes of the galaxy 3C275 in the cluster A400.

Blasi 1998, Colafrancesco et al. 2006 and references therein), while they can diffuse out of galactic and sub-galactic structures (see e.g. Colafrancesco et al. 2007).

Radio observations and Magneto-hydrodynamic (MHD) simulations also suggest that large scale **magnetic fields** (of

either primordial origin or post-recombination generation, see e.g. Giovannini 2004 for a review) are associated to the distribution of baryonic material collected in LSS potential wells (see e.g. Sigl et al. 2005, Dolag et al. 2005). The seed magnetic field is likely amplified and made turbulent by the coupling

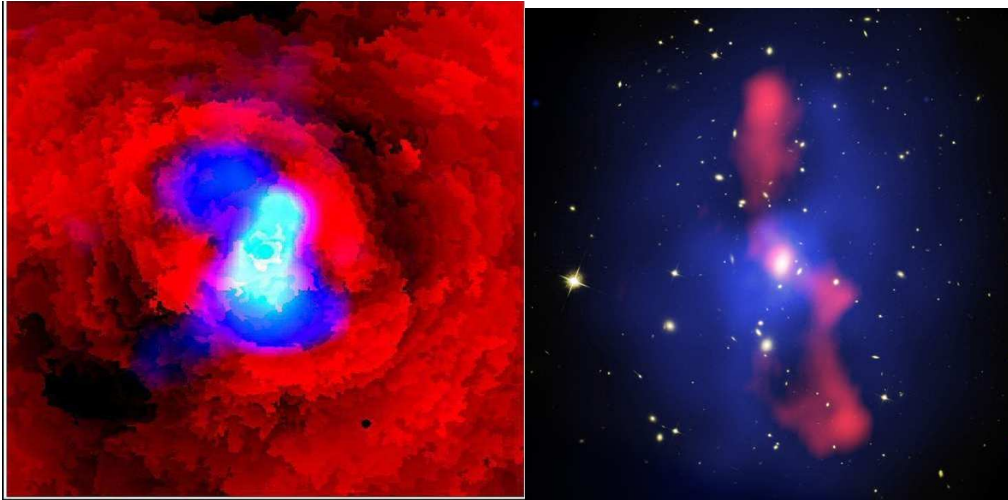


**Fig. 3.** Left. A composite X-ray and radio image of the Perseus cluster (from Fabian & Sanders 2006). Right. A composite X-ray (blue) and radio (magenta) image of the cluster MS 0735+7421 (McNamara et al. 2000. Credit: X-ray: NASA/CXC/Univ. Waterloo/B.McNamara; Optical: NASA/ESA/STScI/Univ. Waterloo/B.McNamara; Radio: NRAO/Ohio Univ./L.Birzan et al.).

of gravitational collapse and MHD processes during the formation of galaxy clusters. Evidence for such wide-scale and turbulent intra-cluster magnetic field is indicated by the diffuse radio synchrotron emission found in many nearby clusters (with typical values  $B \sim 0.1 - 2 \mu\text{G}$ ), by radio relic features in dynamically active clusters (with typical values  $B \sim 0.2 - 5 \mu\text{G}$ ) and by Faraday Rotation measurements of background and embedded polarized radio sources (with typical values  $B \sim 1 - 50 \mu\text{G}$ , Carilli & Taylor 2001, Govoni & Feretti 2005).

Very massive DM clumps that collapse at high redshifts ( $z \sim 6 - 7$ ) often contain the most massive **Black Holes** (BHs) at their centers (see, e.g., results from the Millennium simulation, Springel et al. 2005). The AGN descendants of these ancient supermassive BHs (SMBHs) are found to be part of the massive galaxies located at the centers of the most massive galaxy clusters we observe at the present epoch. We know, in fact, that massive radio galaxies and blazars are often found in the cores of galaxy clusters (like, e.g., CenA, M87/Virgo, Perseus, A262, A4059) with their radio lobes penetrating the ICM for tens or

hundreds of kpcs. It is often observed that the radio jets/lobes end up in approximately spherical **bubbles of relativistic plasma** (likely containing relativistic or mildly-relativistic plasmas) that appear as cavities in the X-ray images of galaxy clusters (see e.g. Birzan et al. 2004) with dimensions ranging from a few kpcs (as in Perseus) to  $\sim 100$  kpc (as in the case of the cluster MS0735-556, McNamara & Nulsen 2007). The combination of high-resolution radio and X-ray images indicates that the relativistic plasma found inside the X-ray cavities is connected with the jet/lobe structure of the central AGN and with the history of the ejection events and mechanisms from the central AGN (see Fig.3). The cores of galaxy clusters which host such non-thermal phenomena (BHs, cavities, high magnetic fields, see Eilek & Owen 2006) are found to be systematically cooler than the outer regions of the clusters with the inner temperature setting at a value  $\sim \frac{1}{3} - \frac{1}{2}$  of the outer temperature, usually consistent with the virial expectation (see Colafrancesco 2008a and Colafrancesco & Marchegiani 2008 for a discussion and references to Chandra and XMM observations). It seems that a heating agent of

non-gravitational and non-thermal nature – with a heating rate that is able to accommodate itself to the cooling rate of the intra-cluster plasma – is present in the cluster's **cool core** so as to maintain it in a quasi-stationary, warm configuration (Colafrancesco, Dar & DeRujula 2004, Colafrancesco & Marchegiani 2008).

The previous evidence indicates that galaxy clusters – the largest bound structures in the universe and the pillars of the LSS distribution – are the largest storage rooms for cosmic material (galaxies, DM, hot thermal baryonic plasma, non-thermal and relativistic plasma, BHs, magnetic fields, CRs). In this sense they can be considered as the largest multi-disciplinary laboratories for Astro Particle Physics in the universe. In such laboratories one can efficiently study some of the most interesting aspects of the astro-particle physics of LSS: the nature of DM, the origin and distribution of CRs, the impact of magnetic fields on LSS, the impact of BHs on LSS, the interplay between thermal and non-thermal phenomena in LSS.

The wide range of physical phenomena occurring in LSS requires a multi-disciplinary approach for studying their origin and evolution: astrophysical information must be combined with fundamental physics information as well as with magneto-hydrodynamical plasma physics to provide a consistent picture of the condensates in our universe.

Such a multi-disciplinary approach must be further set to the probes of a multi-frequency analysis of the various emission mechanism related to the previous phenomena.

We will discuss in the following some of the results obtainable along these lines of investigation.

## 2. Multi-frequency vs. multi-discipline

The phenomenology of galaxy clusters (and more generally of LSS) previously discussed indicates that a complex leptonic distribution is present in their atmospheres: the superposition of electron populations of thermal, non-thermal, mild and fully relativistic nature provides a set of emission spectra spread over the whole electromagnetic (e.m.) spectrum, from

radio to gamma-rays. A multi-frequency analysis is, therefore, optimally suited to disentangle the various components of the clusters' lepton (and hadron) distribution and is able, in principle, to provide a detailed tomography of the atmospheres of galaxy clusters, and more generally of LSS. In the following, we will discuss how a multi-frequency analysis of the e.m. signals visible from galaxy clusters is able to provide relevant information on the multi-disciplinary aspects of the physics of LSS.

To this aim we discuss specifically two different clusters as examples of our analysis: Ophiuchus and Perseus.

The Ophiuchus cluster is an almost isothermal cluster with a single temperature of  $T \sim 9.5$  keV, no-cool core, no AGN in the core, and a radio halo found at  $\nu = 1.4$  GHz. For this reason it is a good laboratory to test the DM, CRs, WRs and B-field distribution in LSS.

The Perseus cluster is a multi-temperature structure with a well-defined cool core (CC), an AGN-dominated core, a mini radio halo, and a complex distribution of non-thermal plasma. For this reason it is an optimal laboratory to test DM, CRs, WRs, B-field distribution and their relation to the central super massive BH.

### 2.1. Ophiuchus cluster

The Ophiuchus cluster is an almost isothermal cluster with a single temperature of  $T \sim 9.5$  keV, no-Cool Core, no AGN in the core, and a radio halo detected at  $\nu = 1.4$  GHz.

The puzzling HXR emission excess detected from Ophiuchus (Eckert et al. 2008 for INTEGRAL observation, Ajello et al. 2009 for Swift-BAT observation) has been interpreted as ICS emission from either a population of primary cosmic ray electrons (Eckert et al. 2008) or secondary electrons produced in neutralino DM annihilation (Profumo 2008). In particular, Profumo (2008) proposed that a combination of three different neutralino  $\chi$  DM models [ $M_\chi = 81(W^+W^-)$ ,  $40(b\bar{b})$  and  $10(\tau^+\tau^-)$  GeV] is consistent with all non-thermal emission data for Ophiuchus, from radio to gamma-rays.

The available data on diffuse radio emission in the core of Ophiuchus and the overall analysis of its multi-frequency spectral energy distribution (SED) further led Perez-Torres et al. (2008) to conclude that i) a synchrotron+ICS model from primary cosmic ray electrons is in marginal agreement with the available data, for a range of magnetic field values  $B \sim 0.02 - 0.3 \mu\text{G}$ ; ii) that a pure neutralino annihilation scenario cannot reproduce both radio and HXR emission, unless extremely low magnetic field values ( $10^{-2}$  to  $10^{-3} \mu\text{G}$ ) are assumed; iii) a scenario in which synchrotron and ICS arise from PeV electron-positron pairs (via interactions with the CMB), can also be excluded, since it predicts a non-thermal soft X-ray emission that largely exceeds the thermal bremsstrahlung emission measured by INTEGRAL.

However, it has been shown by Colafrancesco & Marchegiani (2008) that a more radical approach to the problem of the HXR emission of Ophiuchus must be taken and consider not only the SED properties of synchrotron plus ICS scenarios (from both primary and secondary electrons) but also the physical consequences of the ICS origin of the HXR emission in all models so far viable: primary electron model, secondary electron models from pp collisions and from DM annihilation, and finally a Warming Ray model.

It has been demonstrated (Colafrancesco & Marchegiani 2008) that various problems exist with the ICS interpretation of the HXR excess emission from the Ophiuchus cluster and, in general, of galaxy clusters for which an HXR emission excess has been detected. These problems are:

i) The true level of the HXR emission flux. The derivation of an HXR emission excess in clusters seems to depend strongly on the precise determination of the background thermal bremsstrahlung emission. In fact, using INTEGRAL data, Eckert et al. (2008) derived an HXR flux in the 20–60 keV band of  $F_{\text{HXR}} = (10.1 \pm 2.5) \times 10^{-12} \text{ erg cm}^{-2} \text{ s}^{-1}$ , for an IC gas temperature of  $8.56^{+0.37}_{-0.35} \text{ keV}$ . Using Swift BAT data, Ajello et al. (2009) derived an upper limit (90% c.l.) of  $F_{\text{HXR}} \leq 7.2 \times 10^{-12} \text{ erg}$

$\text{cm}^{-2} \text{ s}^{-1}$ , for a different IC gas temperature of  $9.5^{+1.4}_{-1.1} \text{ keV}$  (the same authors derived an upper limit to the HXR flux of  $F_{\text{HXR}} \leq 4.5 \times 10^{-12} \text{ erg cm}^{-2} \text{ s}^{-1}$  by using a higher value of temperature  $9.93^{+0.24}_{-0.24} \text{ keV}$ , obtained by using a combination of Chandra and Swift-BAT data).

In conclusion, it is clear that a crucial input quantity in determining the value of the HXR excess flux is the detailed modeling of the thermal emission of the IC gas, because different values assumed for the IC gas temperature lead to different conclusions about the amount of HXR excess flux (references about the long standing discussion on the evidence and counter evidence of the HXR excess in Coma can be found in Colafrancesco & Marchegiani 2009; see also Petrosian et al. 2008 for a review). For this reason, it would be extremely important to estimate the temperature of the IC gas with measurements that are independent of those obtained in the X-ray band. In this context, we note that a reliable method of measuring IC gas temperatures can be found by using Sunyaev-Zel'dovich effect (SZE) observations over a wide spectral band (from  $\sim 100$  to  $\sim 400 \text{ GHz}$ ) reaching high frequencies where the sensitivity of the SZE to the cluster temperature is maximal (see Colafrancesco & Marchegiani 2009; see also Colafrancesco et al. 2003, Colafrancesco 2009b,c and Colafrancesco 2007 for a review).

ii) The ICS HXR scenario. The hypothesis that high-E electrons are responsible for an ICS HXR emission at the level found by Swift-BAT and INTEGRAL observations leads to some important consequences.

First, to reconcile the HXR excess value with the relative diffuse synchrotron radio emission (from the same electron population) at the level observed in the same cluster, the value of the average magnetic field must be quite low and of the order of  $\sim 0.1 \mu\text{G}$  for  $p = 3.5$  and  $\sim 0.2 \mu\text{G}$  for  $p = 4.4$  (see Fig. 4). The result found for Ophiuchus is analogous to that derived for other clusters (see also our previous results discussed in Colafrancesco, Marchegiani & Perola 2005, Marchegiani, Perola & Colafrancesco 2007). Specifically, the Ophiuchus data are consistent with an IC magnetic field of order  $\sim 0.7$  and

1.2  $\mu\text{G}$  at the cluster center with a decreasing radial profile similar to that of the IC gas, for  $p = 3.5$  and 4.4, respectively.

Secondly, there is a strong relation between the ICS HXR emission level and the relative gamma-ray emission and the consequences on the physics of the cluster, i.e., the heating of the IC gas and the ratio of non-thermal to thermal pressures:

- if the electrons producing the HXR emission are primaries, their gamma-ray emission (dominated at  $E < 1$  GeV by non-thermal bremsstrahlung) is slightly lower than the EGRET upper limit in the  $p = 3.5$  model, and slightly higher than this limit in the  $p = 4.4$  model, but certainly detectable by Fermi (see Fig.5). If Fermi does not detect this gamma-ray emission, one should conclude that the ICS HXR emission is much lower than the Swift-INTEGRAL HXR detection and that the relativistic electron content of Ophiuchus is consequently much lower. The HXR data imply, in addition, a cut-off of  $E_{min} \sim 33$  and 93 MeV (for  $p = 3.5$  and 4.4) on the electron spectrum in order to maintain the heating rate below the cooling rate;

- if the electrons responsible for the ICS HXR emission are secondary particles produced in the decay of charged pions generated by cosmic-ray proton collisions with the IC gas protons (SEM-pp), then an ICS flux set at the HXR observations has unacceptable consequences. Specifically, we find that: in the  $s = 2.5$  case, the pressure exerted by relativistic protons at the cluster center is  $\sim 5$  times higher than the thermal gas one; the heating rate induced by the same relativistic protons at the cluster center is  $\sim 23$  times higher than the IC gas cooling rate; and the gamma-ray emission produced by neutral pion decay exceeds the EGRET limit by a factor  $\sim 18$ ; in the  $s = 3.4$  case, these quantities increase to  $\sim 367$ , 298, and 170, respectively (see Fig. 6). For all these reasons, we conclude that if electrons produce an ICS HXR emission in the observed range, they cannot be secondary (in the SEM-pp). This conclusion is analogous to that found for other clusters like Coma, A2199, A2163, and Perseus (see Colafrancesco & Marchegiani 2008);

- if electrons are produced by neutralino DM annihilation, we have found that: the heating rate they induce at the cluster center is quite high (see Colafrancesco & Marchegiani 2009); the relative gamma-ray emission exceeds the EGRET limit for the two high- $M_\chi$  models considered here ( $M_\chi = 40$  and 81 GeV) (see Fig. 7), with a marginal consistency for the low-mass model with  $M_\chi = 10$  GeV; the radio flux produced by electrons is consistent with the available data for  $M_\chi > 40$  GeV, and for  $B < 0.18 \mu\text{G}$ . Therefore, the information inferred by gamma and radio data are not compatible, and we conclude that it is not possible to conceive that the ICS HXR emission of secondary SEM-DM electrons has a flux close to that of the available observations (i.e., the maximum allowed flux set by Swift and INTEGRAL), and thus their annihilation cross-section must be much lower than the values used by Profumo (2008). Even normalizing these models to the lower allowed flux value of the HXR excess of Ophiuchus, all the previous results vary (decrease) by  $\sim 15\%$ , leaving our basic conclusions unchanged.

- iii) Relaxing the assumption of recovering the observed HXR excess and assuming that non-thermal protons act as warming rays (see Colafrancesco & Marchegiani 2008), it is possible to paint a much more acceptable scenario in which the unacceptable pressure ratios derived in SEM models do not hold since the ratio  $P_{non-th}/P_{th} \approx 0.17$  and 1.0 for  $s = 2.5$  and 3.4, respectively, and is constant throughout the cluster (this is because non-thermal protons must have the same spatial distribution as the thermal IC gas to recover the spatial temperature distribution of the cluster). The WR model has other positive aspects for the cluster structure: i) it does not induce excess heating effects, since a quasi-stationary balance between heating and cooling is the working assumption of the WR model; ii) we found that the diffuse radio emission produced in this case requires, for  $s = 2.5$  and  $s = 3.4$  respectively, a value of the average magnetic field of  $\sim 0.4$  and 2  $\mu\text{G}$  (see Fig. 8) and a central value of  $\sim 1.1$  and 6  $\mu\text{G}$  with a radial profile similar to that of the IC gas, which is consistent with the general findings for clusters with Faraday Rotation

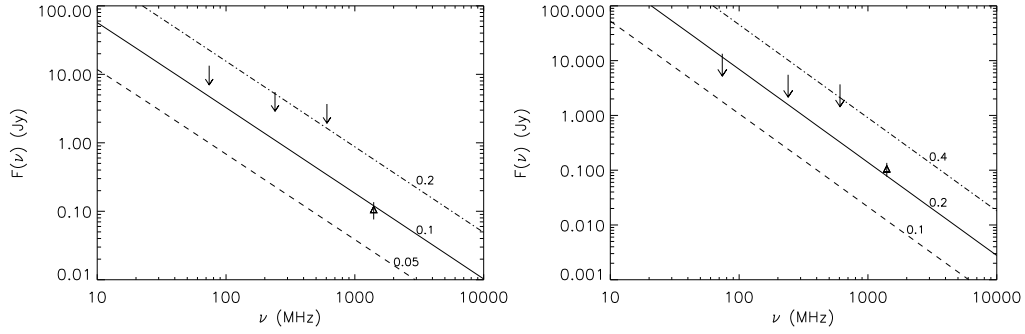


**Fig. 4.** The diffuse radio-emission spectrum produced by primary electrons with  $p = 3.5$  (upper panel) and  $p = 4.4$  (lower panel) is shown for different values of the uniform magnetic field (in units of  $\mu\text{G}$ ), as labelled. Data are from Perez-Torres et al. (2008) (upper limits) and Govoni et al. (2009) (point at 1.4 GHz).

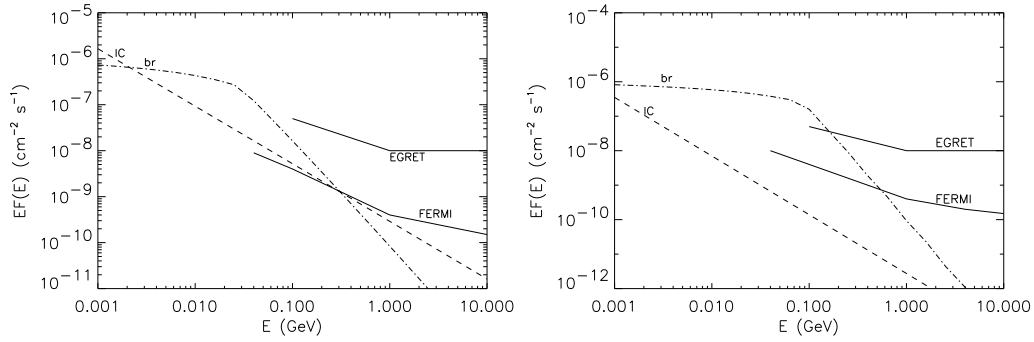


**Fig. 5.** The gamma-ray spectrum produced by primary electrons with  $p = 3.5$  (upper panel) and  $p = 4.4$  (lower panel) via ICS (dashed) and bremsstrahlung (dot-dashed) are compared to the sensitivity curves of EGRET and Fermi ( $5\sigma$ , 1 year observation).

measurements (see, e.g., Carilli & Taylor 2002, Govoni & Feretti 2004); iii) the gamma-ray emission produced in this model is considerably lower than the EGRET limit but definitely detectable by Fermi (see Fig. 8). The Fermi detection of this gamma-ray emission from Ophiuchus will have a crucial impact in proving or disproving this model.

In the WR model, the HXR ICS flux of Ophiuchus is much lower (by a factor  $\sim 30$  and 362 for  $s = 2.5$  and  $s = 3.4$ , respectively) than the limit set by the present observations (by INTEGRAL and Swift-BAT) and could only be detectable by using long-exposure obser-

vations with the next generation HXR instruments like NeXT (see e.g., Takahashi et al. 2004).

To conclude, models of high-E electrons that can be adjusted to reproduce the cluster ICS HXR emission at the level indicated by the available observations fail to work because they would imply unacceptable levels of heating and gamma-ray emission (Colafrancesco & Marchegiani 2009). In contrast, models of high-energy particles that are able to reproduce the IC gas temperature structure (i.e., the WR model) predict a level of non-thermal HXR ICS emission that is far below the current ex-

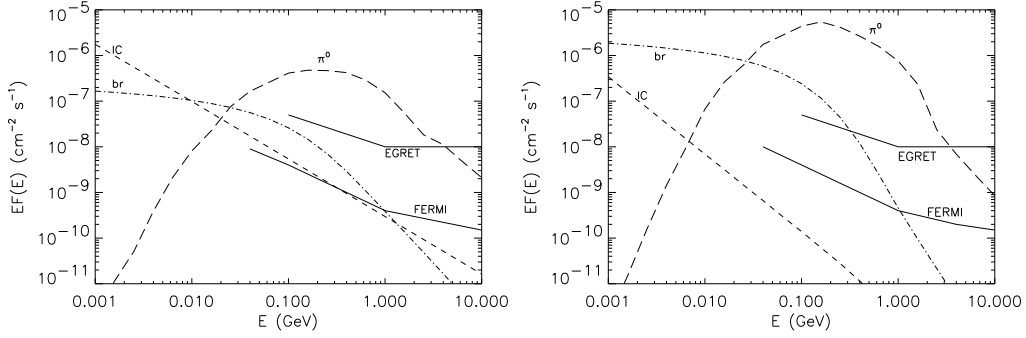


**Fig. 6.** The gamma-ray spectrum of Ophiuchus with  $s = 2.5$  (upper panel) and  $s = 3.4$  (lower panel) produced by ICS (dashes) and bremsstrahlung (dot dashes) of secondary electrons and by neutral pion decay (long dashes). The predictions of the SEM-pp model are compared to the sensitivity curves of EGRET and Fermi ( $5\sigma$ , 1 year observation).

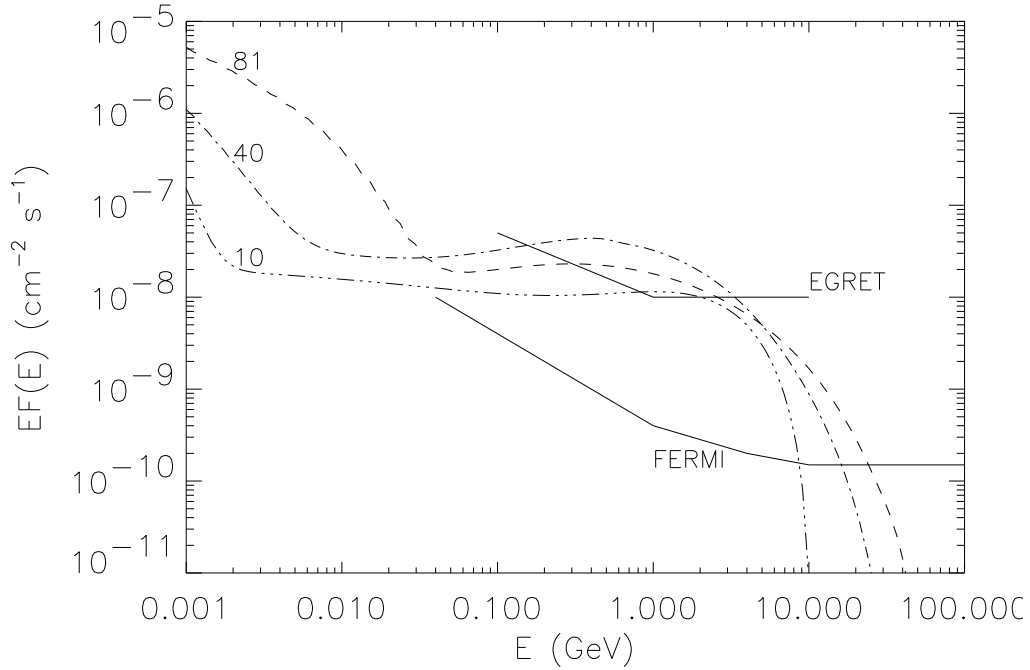


**Fig. 7.** The overall gamma-ray spectrum produced by the composition of the contributions of the secondary SEM-DM electrons (ICS and bremsstrahlung) and of the neutral pion decay for the three neutralino models here considered. The sensitivity curves of EGRET and Fermi ( $5\sigma$ , 1 year observation) are shown for comparison.

perimental limits, and provide an overall SED that is consistent with all the available data –

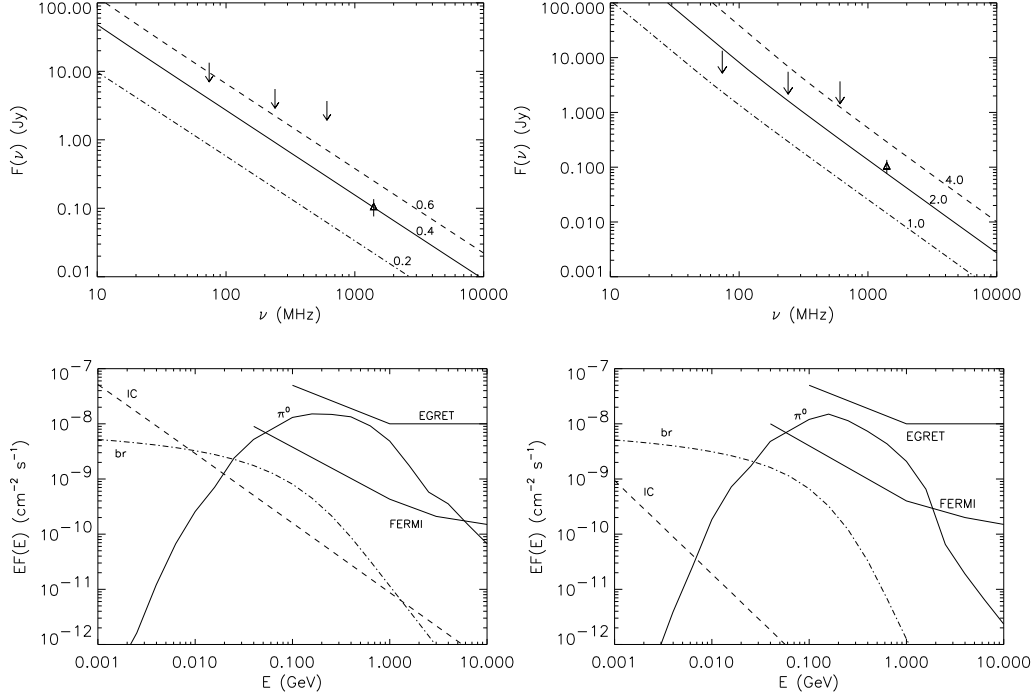


**Fig. 8.** The radio halo spectrum produced by secondary electrons with  $s = 2.5$  (upper left panel) and  $s = 3.4$  (upper right panel) in the WR model is shown for different values of a constant IC magnetic field (as labeled) in units of  $\mu\text{G}$ . Data are from Perez-Torres et al. (2008) (upper limits) and Govoni et al. (2009) (point at 1.4 GHz). The gamma-ray spectrum produced by secondary electrons with  $s = 2.5$  (upper panel) and  $s = 3.4$  (lower panel) via ICS (dashes) and bremsstrahlung (dot-dashes) and neutral pion decay (solid) in the WR model constrained to reproduce the observed temperature structures of the IC gas in Ophiuchus. The sensitivity curves of EGRET and Fermi ( $5\sigma$ , 1 year observation) are shown for comparison.

from radio to gamma-rays – for Ophiuchus as well as for other clusters.

## 2.2. The Perseus cluster and NGC 1275

The Perseus cluster is a multi-temperature structure with a well-defined cool core (CC) with a powerful radio galaxy NGC 1275 at its center, a mini radio halo, and a complex distribution of thermal and non-thermal plasma. For this reason it is an optimal laboratory to test DM, CRs, WRs, B-field distribution and their relation to the central super massive BH.

The radio-galaxy NGC 1275 (3C 84) has been recently detected by *Fermi* as a source

of high-energy gamma rays with an average flux  $F(> 100 \text{ MeV}) = (2.10 \pm 0.23) \times 10^{-7} \text{ cm}^{-2} \text{ s}^{-1}$  and power-law photon index  $\gamma = 2.17 \pm 0.05$ , respectively (Abdo et al. 2009). The emission detected by the *Fermi*-LAT is consistent with a point source centered at the nucleus of NGC 1275. The gamma-ray flux measured with *Fermi*-LAT is almost an order-of-magnitude brighter than the EGRET flux upper limit,  $F(> 100 \text{ MeV}) < 3.72 \times 10^{-8} \text{ cm}^{-2} \text{ s}^{-1}$ , and therefore implies that NGC 1275 is varying significantly at gamma-rays on yr. time scales.

The *Fermi* results on NGC1275 have clearly an impact on the models for the possi-

ble gamma-ray emission originating from the surrounding Perseus cluster atmosphere because they limit the amount and the SED of the diffuse gamma-ray emission that can originate from the hosting galaxy cluster.

The Perseus cluster (as many other galaxy clusters) is indeed expected to be a source of gamma-ray emission due to various emission mechanisms (see e.g., Colafrancesco 2007, 2008a, 2009a-d for reviews and references to the subject): i) Inverse Compton Scattering (ICS) of CMB photons and relativistic bremsstrahlung of primary cosmic ray particles (mainly electrons); ii) neutral pion e.m. decay,  $\pi^0 \rightarrow \gamma\gamma$ , produced by pp collisions, and ICS of CMB photons and relativistic bremsstrahlung of secondary electrons produced in the same pp collisions; iii) neutral pion e.m. decay produced by Warming Rays interaction and ICS of CMB photons and relativistic bremsstrahlung of secondary electrons produced in the same pp collisions; iv) neutral pion e.m. decay produced by neutralino DM annihilation, and ICS of CMB photons and relativistic bremsstrahlung of secondary electrons produced in the same DM annihilation processes; v) ICS and relativistic bremsstrahlung from PeV electron-positron pairs produced via interactions of Ultra High Energy photons (particles) with the CMB photons.

Experimental limits on the gamma-ray emission from the Perseus cluster have been obtained also by other experiments beyond EGRET. Limits on TeV emission at  $E > 400$  GeV have been obtained with Whipple ( $F < 7.4 \times 10^{-12}$  erg cm $^{-2}$  s $^{-1}$ ; see Perkins et al. 2006) and from MAGIC at  $E > 100$  GeV ( $F < 4.6$  to  $7.5 \times 10^{-12}$  cm $^{-2}$  s $^{-1}$ , for spectral indices in the range  $-1.5$  to  $-2.5$ ; see Aleksic et al. 2009). Very recently, a new upper limit has been obtained with VERITAS (Acciari et al. 2009), with  $F(> 188$  MeV)  $< 5.11 \times 10^{-12}$  cm $^{-2}$  s $^{-1}$  while the source was in a quite low state at the gamma-ray energies probed by *Fermi*. At soft gamma-ray energies, INTEGRAL observations of the Perseus cluster found no evidence for a diffuse power-law emission which would dominate the emission above 30 keV (Eckert & Paltani 2009).

However, the angular resolution of IBIS/ISGRI is not sufficient to disentangle the point-like emission from the diffuse component, so it is not possible to set any definite upper limit on the diffuse non-thermal emission. Swift-BAT observations of the nucleus of Perseus cluster (Ajello et al. 2009) revealed an hard X-ray tail that is most likely associated to NGC 1275 than to a non-thermal component originated in the intracluster medium (ICM). The nucleus of Perseus displays also a moderate variability between the XMM-Newton and Swift/XRT observation epochs (Ajello et al. 2009). This further supports the interpretation that the non-thermal emission of hard X-rays and of the gamma-rays is mostly produced by the central AGN.

At the same time, several theoretical predictions on the intensity and spectral properties of the Perseus cluster gamma-ray emission have been presented. Pfrommer (2008) predicted a total gamma-ray flux at  $E > 100$  MeV that is in the range  $(3.2 - 5.6) \times 10^{-9}$  cm $^{-2}$  s $^{-1}$  depending on the details of their models of relativistic electrons accelerated at cosmological structure formation shocks and those that are produced in hadronic interactions of cosmic rays with ambient gas protons. Kushnir & Waxman (2009) predicted, in a simple model that explains the HXR emission from galaxy clusters as ICS scattering of CMB photons by relativistic electrons accelerated at the accretion shock surrounding the cluster, a gamma-ray flux for Perseus (within 0.1 deg) at  $E > 50$  GeV of  $3.1 \times 10^{-13}$  cm $^{-2}$  s $^{-1}$  for the pion decay channel production, and of  $1.5 \times 10^{-13}$  cm $^{-2}$  s $^{-1}$  for the ICS channel production. Colafrancesco & Marchegiani (2008) predicted that the simplest WR model should produced a total (maximal) gamma-ray flux for Perseus (integrated within its virial radius) of  $1.2 \times 10^{-8}$  cm $^{-2}$  s $^{-1}$  at  $E > 100$  MeV.

In a system in which gamma-ray emission is expected by both the central AGN and by the surrounding diffuse cluster atmosphere the understanding of the nature of the central radio galaxy SED (and especially of its high-E branch at  $E \gtrsim$  GeV) is crucial in setting more precise constraints to the amount of diffuse gamma-ray emission of the Perseus clus-

ter, and hence to the SED of the cluster non-thermal emission models; in this respect, such a knowledge guides in outlining the optimal strategy for the detectability of galaxy clusters at gamma-ray energies.

The gamma-ray emission features of the combined system of NGC 1275 living in the core of the Perseus cluster have been studied in a multi-component model (the Cannon Model, see Colafrancesco & Marchegiani 2010) and in a multi-frequency approach (Colafrancesco et al. 2010). Such study provides various constraints on the NGC 1275 emission properties, on the cluster atmosphere, and on the interaction of the two sources. In this context, it helps to assess a strategy able to disentangle the gamma-ray emission of the cluster from that of the galaxy NGC1275.

The Cannon Model (CM) (Colafrancesco & Marchegiani 2010) for NGC 1275 is able to reproduce the *Fermi* observations, the variability of this source in gamma-rays and X-rays, and the different observed intensity states of its multi-frequency SED (see Figs. 9). The results of this study is that the *Fermi* detection of NGC 1275 is entirely due to the emission of a compact ( $r \sim 8 \times 10^{-3}$  pc) and energetic blob of plasma filled with an electron population with double power law spectrum with  $\gamma_b \approx 5 \times 10^3$ , with  $\delta \approx 8$  and relatively high normalization factor  $N \approx 6.8 \text{ cm}^{-3}$ . The SED of this blob perfectly fits the *Fermi* spectrum and is also consistent with MAGIC and WHIPPLE upper limit at TeV energies. We note that the upper limit obtained by VERITAS (Acciari et al. 2009) is lower than the flux of the high-energy component of the CM model (see Fig.9). However, Acciari et al. (2009) pointed that the *Fermi* flux measurements simultaneous with the VERITAS ones are lower by a factor of  $\sim 1.37$  w.r.t. the data of Abdo et al. (2009). Therefore, the VERITAS upper limits are consistent with the fact that they have been measured while the central source was decreasing its high-energy flux, and are hence completely consistent with a variable high-E component of the NGC 1275 SED as predicted by the CM model.

For the surrounding Perseus cluster atmosphere, DM annihilation models with high nor-

malization are excluded because they produce a stationary gamma-ray flux of the same order of that observed at  $E \sim 3$  GeV by *Fermi* from NGC 1275, and produce a spectrum of gamma-ray emission that is strongly peaked at a few GeV, contrary to the spectral shape of the gamma-ray source detected by *Fermi* (see Fig.9).

The WR model produces a gamma-ray flux always much lower (by a factor 5 to 10) than the gamma-ray flux from NGC 1275 observed by *Fermi*.

Due to the fact that the gamma-ray emission of NGC 1275 is variable, it is therefore possible to reveal the diffuse gamma-ray emission from Perseus during a state of low activity of NGC 1275. In the core of the Perseus cluster, the diffuse gamma-ray flux at  $E > 100$  MeV from the cluster atmosphere (both in the WR model and in the unrealistic DM annihilation model with the highest normalization, that produces an over-heating at the cluster center) could be detected by *Fermi* if NGC 1275 is found in a low-state as that produced by the first blob in our CM model (see Fig.9 and Colafrancesco et al. 2010 for details). The diffuse gamma-ray flux coming from these diffuse components might be marginally detectable by CTA at  $E \gtrsim 10$  GeV. The gamma-ray flux produced by DM annihilation with the lowest normalization is undetectable by both *Fermi* and CTA being its peak flux at  $\sim 1$  GeV more than a factor 300 below the *Fermi* (1 yr.,  $5\sigma$ ) sensitivity.

An alternative approach to disentangle the cluster gamma-ray emission from that of NGC 1275 is to determine the diffuse flux outside the cluster core where the emission from the central galaxy is no longer contaminating the measurements. At  $E > 1$  GeV the *Fermi* 68% collecting angle is  $\sim 0.6$  deg. that corresponds to  $\sim 786$  kpc from the cluster center: thus *Fermi* can have the possibility to resolve and detect the diffuse gamma-ray flux coming from the outer corona of the Perseus cluster atmosphere at distances  $r \gtrsim 800$  kpc from the center of the cluster. The gamma-ray flux from Perseus evaluated in the corona between 0.786 and 1 Mpc (i.e., approximately the largest radius to which X-ray thermal emission is ob-

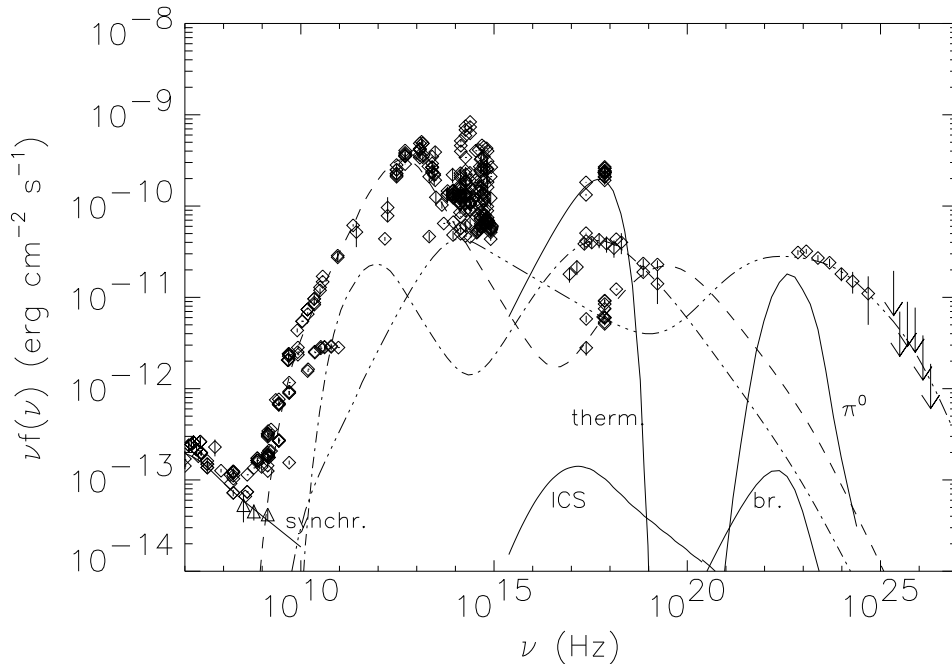


**Fig. 9.** The three SSC components needed to recover the full SED of NGC 1275 are compared with the various diffuse emission components (as labelled) of the Perseus cluster in the WR model (solid curves).

served) is  $F(> 1 \text{ GeV}) \approx 1.2 \times 10^{-10} \text{ cm}^{-2} \text{ s}^{-1}$  in WR model, which can be marginally detectable from *Fermi*. Therefore, such a strategy could provide a likely detection of the diffuse gamma-ray emission from the Perseus cluster.

This argument does not apply to the case of DM models because in such a case the gamma-ray flux comes mainly from the inner cluster region due to the  $\propto n_{DM}^2(r)$  dependence of the annihilation flux. This implies that a spatially resolved observation of the Perseus cluster in gamma-rays cannot provide information on the DM models since the relative gamma-ray brightness is not observable at large angular distances from the central galaxy.

As for the full multi-frequency approach we find that the diffuse emission produced in the cluster core is much less than that of the central galaxy with the exception of two frequency windows: the radio frequency region

at  $\nu \lesssim 1 \text{ GHz}$  in which the diffuse mini radio halo of Perseus dominates the emission, and the soft X-ray band ( $E \sim \text{keV}$ ), in which the thermal emission from the cluster gas peaks (see Colafrancesco et al. 2010).

The WR model is the one that better fits both the mini radio halo features (requiring a magnetic field radial profile almost constant in the cluster core  $R \leq 215 \text{ kpc}$  and with a value of  $B \sim 4 \mu\text{G}$ , consistently with Faraday Rotation measurements, see Carilli & Taylor 2002) and the flux and temperature distribution of the diffuse, X-ray emitting plasma. DM annihilation models produce, instead, a much steeper density profile towards the cluster center and might then reproduce the radio halo brightness profile only for a B-field radial profile which rapidly increases towards the outer cluster regions.

We have also considered the gamma-ray emission produced by a population of relativis-

tic electrons (directly accelerated by intracluster shocks or by turbulence) that have an equilibrium energy spectrum given by  $N_e \propto E^{-p}$ , with  $p = 3.7$  such that the spectral shape of the mini radio halo in Perseus can be reproduced. As for the normalization of the electron spectrum, we considered two different cases:

i) the electron density is normalized to reproduce the *Fermi* gamma-ray flux with their non-thermal bremsstrahlung emission. This condition implies that the electron spectrum must have a break at an energy  $E \sim 150$  MeV in order to have a heating rate smaller than the thermal bremsstrahlung cooling at the cluster center. With such a spectrum, the gamma-ray emission produced by these electrons is dominated up to  $E \sim 4$  GeV by the bremsstrahlung emission component, that has a spectral shape different from that of the *Fermi* data. The multi-frequency behaviour of this electron spectrum implies that in the 2 – 10 keV band the relativistic electrons produce a ICS-on-CMB flux of  $4.8 \times 10^{-11}$  erg cm $^{-2}$  s $^{-1}$ , smaller than the flux  $6.3 \times 10^{-11}$  erg cm $^{-2}$  s $^{-1}$  estimated by Sanders et al. (2005) from the center of Perseus. The same electron population might reproduce the mini radio halo flux of Perseus assuming a central magnetic field  $B_0 \sim 1.5$   $\mu$ G under the assumption that the radial profile of the magnetic field is similar to that of the intracluster gas.

ii) the electron density is normalized to fit the *Fermi* gamma-ray flux with their ICS-on-CMB emission: in this case, the required electron density is  $\sim 60$  times larger than in the previous case and, consequently, the energy scale of the spectral break required to avoid an excessive heating of the thermal gas is  $E \sim 690$  MeV. With such a spectrum, the gamma-ray flux is still dominated by the bremsstrahlung component up to  $E \sim 2$  GeV, and therefore the model is untenable because the total gamma-ray emission (bremsstrahlung plus ICS-on-CMB) is larger than that detected by *Fermi*. The same conclusion is reinforced by the predictions of the multi-frequency behaviour of such electron spectrum: the ICS flux in the 2 – 10 keV band is  $1.3 \times 10^{-9}$  erg cm $^{-2}$  s $^{-1}$ , larger than that measured, and the central value of the magnetic field required to fit the

mini radio halo spectrum is  $\sim 0.25$   $\mu$ G, much lower than the values usually derived for cool core clusters.

In summary, the gamma-ray emission from the Perseus cluster is dominated in its central region by NGC 1275, a situation similar to those found for the first preliminary evidence found with EGRET of gamma-ray emitting clusters hosting powerful radio galaxies (see discussion by Colafrancesco 2002). This seems to be the most promising case to observe galaxy cluster in gamma-rays at the moment, even though the expected detectable number of clusters is quite limited to a few specific cases. These conclusions are certainly quite different from those of other (accreting and merging cluster) models in which it has been predicted that the operating gamma-ray missions should have already discovered a significant number (i.e., 5 to 7 clusters with AGILE, and about 20 clusters with *Fermi*) after 1 yr. operation (see, e.g., Blasi, Gabici & Brunetti 2007).

In conclusion, the results we discuss here show that a simultaneous study of the various emission mechanisms that produce diffuse gamma-rays from galaxy clusters and the study of the emission mechanisms that produce gamma-rays from BH-dominated active galaxies residing in clusters is crucial first to disentangle the spectral and spatial characteristics of the gamma-ray emission, and secondly to assess the optimal observational strategy in the attempt to reveal the still elusive diffuse gamma-ray emission widely predicted for the atmospheres of large-scale structures.

### 2.3. The interplay between BHs & cluster

Intermediate cases between the AGN-dominated, cool-core clusters (like Perseus) and the isothermal clusters (like Ophiuchus) previously discussed are provided by clusters with large cavities that are the late evolutionary stages of galaxy radio lobes expanding and penetrating the hot thermal ICM.

The BH ejecta begin to interplay with the surrounding ICM in the cluster core by creating mini cavities (like in the case of Perseus) which are sites of non-thermal phenomena.

Under specific energetic circumstances, the lobes of the central radio galaxy might penetrate the outer ICM even out to large distances (sometimes even beyond the cluster core, see e.g. the case of the cluster MS0735+7421) where the front of the radio lobes can expand to giant dimensions (of order of  $\sim 10 - 100$  kpc) creating deep ICM cavities that are filled with energetic particles of non-thermal origin. It has been shown that the energy necessary to support the largest cavities observed (like those of Hydra and MS0735+7421) is of the order of  $10^{60} - 63$  ergs, the cavity age must be  $\gtrsim 10^8$  yrs and the particle diffusion coefficient inside the cavity is  $\lesssim 10^{28}$  cm<sup>2</sup>/s (Matthews & Brighenti 2007). Such conditions indicate that the cavities are likely supported by hadronic cosmic rays, while the leptonic component, that suffers faster energy losses, has faded away more rapidly.

In such a scenario (that is a natural outcome of the CM model), one expects that the multi-frequency signatures of cavities provide hints of the long-term interplay of the central SMBH with the cluster ICM. The cavity SEDs emerge from that of the surrounding thermal ICM mainly at radio and gamma-ray frequencies, with a quite weak non-thermal hard X-ray emission tail provided by ICS emission of up-scattered CMB photons. The ICS emission of the CMB photons is more evident in the non-thermal SZE associated to the cluster cavities (see, e.g., Colafrancesco 2005).

### 3. Overall vision: LSS formation and BH feedback

The previous evidence and interpretation lead to an overall vision for the formation of LSS and its pillars, i.e. galaxy clusters, and for the feedback coming from its BHs.

LSS formation is driven, in the standard Cold Dark Matter paradigm, by the collapse of DM halos. Some of the highest density DM clumps, even at high redshift, can host SMBHs whose descendant are today the dominant massive galaxies found at the centers of galaxy and groups clusters. Clusters that do not host such SMBHs and the associated AGNs, also do not have very high density and B-field profiles, and

therefore do not develop, with time, large cool cores. In such systems the feedback from BHs is marginal, if any. Clusters that host SMBHs and the associated AGNs, have high density and B-field that trigger the development, with time, of large cool cores. In these kind of systems the feedback from BHs is substantial and appears in various forms: i) a strong activity of the central AGN with the emission of multiple blobs (as predicted in the Cannon Model of Colafrancesco & Marchegiani 2009) of plasma that interact with the surrounding medium and produce a complex SED (like the case of the Perseus cluster and NGC1275); ii) some of the radio-galaxies (or AGNs in general) that live in low-interacting environments and produce particularly energetic blobs can also produce giant cosmic ray flares, some of which might reach extremely high energies, of order of the maximum CR energies recorded in CR showers reaching the atmosphere (see, e.g., the Auger results). iii) the injection of energetic particles (cosmic rays of leptonic and especially hadronic nature) in the cluster medium provides a Warming Ray feedback to the IC gas cooling and provides the necessary quenching of cooling flows and eventually establish a quasi-stationary equilibrium in which an evolving cool-core is produced (see Colafrancesco et al. 2004, Colafrancesco & Marchegiani 2008); iv) under specific energetic and environmental conditions, some of the energetic blobs emitted by the central AGN can penetrate the cluster atmosphere and expand, losing its internal energy, to form cavities in the ICM. Such cavities can have long lifetimes (as in the case of MS0735+7421) and therefore reach far distances from the production point (reasonably close to the central AGN) where they reach quasi-stationary states and start to interact with the surrounding low-energy, thermal medium, and possibly seed the large-scale intracluster magnetic field.

### 4. An experimental outline

The experimental approach to study the complex-mechanism and wide-frequency emission properties of LSS must be necessary demanding and/or versatile. We envisage two

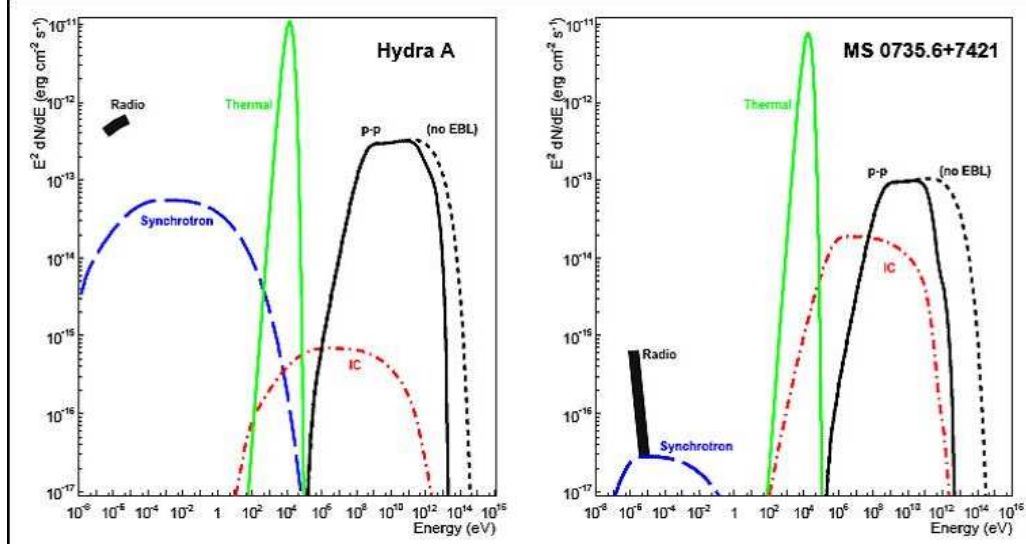


**Fig. 10.** The multi-frequency SED expected from the cavities of Hydra (left) and MS0735+7421 (right). Figures from Hinton et al. (2007).

main approaches:

- the **multi-technique** approach, in which the natural multi-frequency properties of the SEDs of LSS must be tackled by a wide combination, sometimes simultaneous, of experimental efforts with different technological strategies and organized observational campaigns;
- the **single technique** approach, in which one makes use of a single astrophysical effect that is produced by different species of particles, originating and residing in LSS, to define an optimal technological approach devoted to study and disentangle the various astrophysical phenomena at work in LSS.

The first approach requires the canonical multi-frequency study of cosmic structures; the second one requires the use of the CMB photons as the messengers of the multi-disciplinary physical phenomena at work in LSS, as we discuss here below.

#### 4.1. The SZE probes in the atmospheres of LSS

According to the generalized expression for the SZE which is valid in the Thomson limit for a generic electron population, in the full

relativistic treatment and includes also the effects of multiple scatterings and the combination with other electron populations (see Colafrancesco et al. 2003), the spectral distortion observable in the direction of a galaxy cluster is

$$\Delta I(x) = 2 \frac{(k_B T_{CMB})^3}{(hc)^2} y g(x), \quad (1)$$

where the Comptonization parameter  $y$  is given by

$$y = \frac{\sigma_T}{m_e c^2} \int P_e dl, \quad (2)$$

in terms of the pressure  $P_e$  contributed by the specific electron distribution within the cluster. The function  $g(x)$  for the considered electron population can be written as

$$g(x) = \frac{m_e c^2}{\langle k_B T_e \rangle} \cdot \frac{1}{\tau} \cdot \left[ \int_{-\infty}^{+\infty} i_0(xe^{-s}) P(s) ds - i_0(x) \right], \quad (3)$$

in terms of the photon redistribution function  $P(s)$ , of the undistorted CMB spectrum  $i_0(x) =$

$\frac{2(k_B T_{CMB})^3}{(hc)^2} \times \frac{x^3}{(e^x-1)}$ , and of the average energy density

$$\langle \varepsilon \rangle \equiv \frac{\sigma_T}{\tau} \int P_e d\ell = \int_0^\infty dp f_e(p) \frac{1}{3} p v(p) m_e c \quad (4)$$

The photon redistribution function  $P(s) = \int dp f_e(p) P_s(s; p)$  with  $s = \ln(\nu'/\nu)$ , in terms of the CMB photon frequency increase factor  $\nu'/\nu$ , contains the crucial dependence on the electron momentum distribution  $f_e(p)$ , where  $p$  is normalized to  $m_e c$ . Here  $P_s(s; p)$  is the mono-energetic frequency redistribution function.

The spectral function of the SZE evaluated for various electron spectra is shown in Fig.11. It is clear that the different nature of the electron distribution reflects directly in the different spectral shape of the relative SZE. Thus, the SZE is a powerful probe of the energy spectrum of the various electronic populations residing in the atmospheres of cosmic structures. The relevance of the SZE to the study of several different aspects of the astroparticle physics of galaxy clusters has been already addressed by Colafrancesco (2007, 2008b, 2009b,c).

The possibility to study in details the various SZE signals and to extract the relevant astrophysical information depends crucially on the capability to have spatially-resolved spectral observations of LSS over a wide band, from microwaves to mm. In particular, the necessary condition for such study is to have a continuous spectroscopy, a wide-band spectroscopy and especially a good spectral coverage and sensitivity in the high-frequency band, where most of the astrophysical effects reveals more clearly.

The present stage of SZE experiments (e.g., SPT, APEX, ACP), even though they are providing excellent results in terms of imaging and blind search surveys with their low frequency, multiple band observations, do not have neither such spectroscopic capabilities nor a wide and continuous band (and they are not sensitive to the high- $\nu$  range of the SZE signals) over which observations could be performed. Therefore, they can add little to the physical specification of the detected sources and they need X-ray and optical follow-up to

determine the characteristics of the physical parameters extracted from SZE observations.

Due to the rich physical information contained in the SZE (intensity and polarized) signals (of various origin), an effort going from single (or multiple)-band imaging to wide-frequency, continuous spectro-polarimetric imaging is required in order to exploit the physics of the SZE.

Three next coming experiments are on this line.

OLIMPO (Masi et al. 2005) with its four band bolometer array will provide a first survey of SZE sources on arcmin scales from a long-duration stratospheric balloon flight.

SAGACE (Spectroscopic Active Galaxy And Cluster Explorer, see , see also Colafrancesco 2009b,c) will provide the first large area ( $\gtrsim 10^3 \text{ deg}^2$ ) spectroscopic survey of SZE sources in the frequency range  $\sim 100 - 450$  GHz down to  $\sim 10 \mu\text{K}$  sensitivity per pixel.

MILLIMETRON will provide extremely accurate 3-D tomography of SZE sources by using its spectro-polarimetric capability over a wide frequency band ( $\sim 100 - 1000$  GHz) and with unprecedented spatially resolved spectral and polarimetric sensitivity ( $\lesssim 100 \text{ nK}$ ) (see Colafrancesco 2009c).

## 5. Final remarks

The modern Astro Particle Physics view of structure formation poses many fundamental questions on the structure and evolution of LSS that begin to find a theoretical and experimental test bed in galaxy clusters, the largest laboratories for APP in the universe.

Two basic approaches can fulfill this task:

i) a multi-frequency analysis, that requires a combined, challenging synergy from different experiments and different theoretical approaches; ii) a multi-disciplinary approach – which uses the properties of the SZ effect – that is able to probe the physical impact of each particle family and radiation fields through a single experimental, but challenging technique.

The task is anyway demanding but it will return, when achieved, invaluable information on many themes of the present-day Astro Particle Physics research, from the nature of Dark

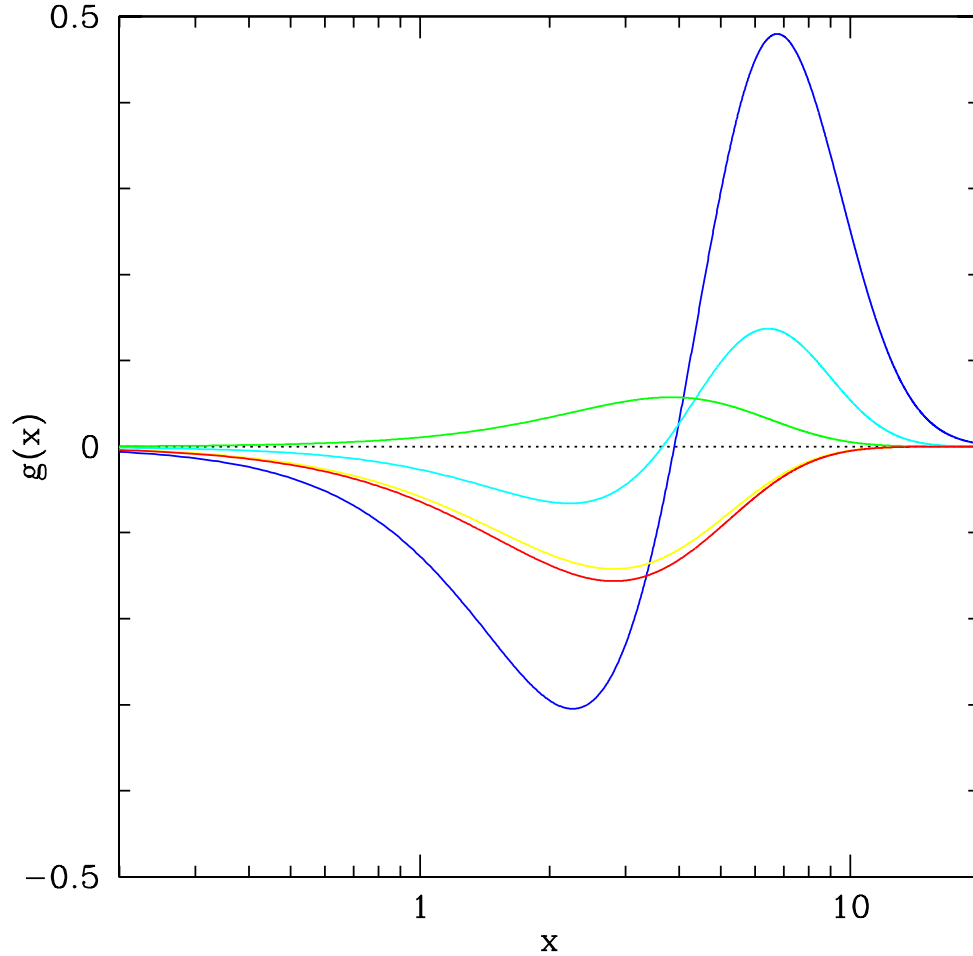


**Fig. 11.** The function  $g(x)$  is shown as a function of the adimensional frequency  $x$  for different electronic populations residing in the cluster atmosphere: thermal with  $k_B T_e = 8.2$  keV (blue); warm with  $k_B T_e = 1$  keV (cyan); secondary electrons from DM annihilation with  $M_\chi = 20$  GeV (red); relativistic electrons which fit the Coma radio halo integrated spectrum (yellow). Also the kinematic SZE with a negative peculiar velocity (green) is shown for comparison. The amplitudes of the various curves have been artificially re-normalized to highlight their frequency dependence.

Matter to the origin of CRs, from the impact and evolution of large-scale B-field to the physical feedback of BHs in cosmic structures. This information is not only precious for its astrophysical impact but is also crucial for the possible cosmological use of galaxy clusters as probes of the structure of the universe.

## References

- Abdo, A. et al. 2009, ApJ, 699, 31
- Acciari, V.A. et al. 2009, ApJL, in press
- Ajello, M. et al. 2009, ApJ, 690, 367

- Aleksic, J. et al. 2009, preprint, arXiv:0909.3267
- Bagchi, J. et al. 2002, arXiv:astro-ph/0204389
- Birzan, L. et al. 2004, ApJ, 607, 800
- Blasi, P., Gabici, S. & Brunetti, G., 2007, Int.J.Mod.Phys., A22, 681
- D. Boyanovsky, H. J. de Vega, N. Sanchez 2007, (arXiv:0710.5180)
- Carilli, C.L. & Taylor, G.B. 2002, ARAA, 40, 319
- Colafrancesco, S., 2002, A&A, 396, 31
- Colafrancesco, S. 2004, A&A, 422, L23
- Colafrancesco, S. 2005, A&A, 435, L9
- Colafrancesco, S. 2007, New Astron.Rev., 51, 394
- Colafrancesco, S. 2008a, *Clusters of galaxies: the largest multi-frequency laboratories for AstroParticle Physics*, CHJAAS, 8, 61
- Colafrancesco, S. 2008b, *Probing cosmology and astro-particle physics with the SZ effect*, invited lecture at the Intl. Conference Problems in Practical Cosmology, Yu.V.Baryshev, I.N.Taganov, P. Teerikorpi eds., Vol.1 TIN, St.Petersburg, Vol.2, ISBN 978-5-902632, p.160-171
- Colafrancesco, S. 2009a, *Dark Matter in modern cosmology*, invited lecture at the 4-th Gamow Intl. Conference "Astrophysics and Cosmology after Gamow: recent progress and new horizons", Odessa (Ukraine)
- Colafrancesco, S. 2009b, invited review at the meeting "CosmoCluster", May 2009, Marseille - France
- Colafrancesco, S. 2009c, Invited review at the Millimetron Meeting, Oct. 2009, Paris - France
- Colafrancesco, S. 2009d, IJMPD, 18, 1541
- Colafrancesco, S. & Blasi, P. 1998, APPhys., 9, 128
- Colafrancesco, S., Marchegiani, P. & Palladino, E. 2003, A&A, 397, 27
- Colafrancesco, S., Dar, A. & DeRujula, A. 2004, A&A, 413, 441
- Colafrancesco, S., Profumo, S. & Ullio, P. 2006, A&A, 455, 21
- Colafrancesco, S. & Giordano, F. 2006, A&A, 454, L131
- Colafrancesco, S., Profumo, S. & Ullio, P. 2007, PhRvD, 75, 3513
- Colafrancesco, S. et al. 2007, A&A, 467, L1
- Colafrancesco, S. & Giordano, F. 2007, A&A, 466, 421
- Colafrancesco, S. & Marchegiani, P. 2008, A&A, 484, 51
- Colafrancesco, S., Prokhorov, D. & Dogiel, V. 2009, A&A, 494, 1
- Colafrancesco, S. et al. 2010, A&A, in press
- Colafrancesco, S. & Marchegiani, P. 2010, A&A submitted
- Dolag, K. et al. 2004, arXiv:astro-ph/0410419
- Eckert, D., et al. 2008, A&A, 479, 27
- Eckert, D. & Paltani, S., 2009, A&A 495, 415
- Eilek, J. & Owen, F. 2006, arXiv:astro-ph/0612111v1
- Fabian, A.C. & Sanders, J.S. 2006, arXiv:astro-ph/0612426
- Fusco-Femiano, R. 2004, Ap&SS, 294, 37
- Govoni & Feretti, L. 2004, IJMPD, 13, 1549
- Giovannini, M. 2004, Int.J.Mod.Phys., D13, 391-502
- Jungman, et al. 1996, Phys. Rep., 267, 195
- Hinton, et al. 2007, preprint arXiv:astro-ph/0701033v3
- Kushnir, D. & Waxman, E., 2009, JCAP, 8, 2
- Marchegiani, P., Perola, G.C. & Colafrancesco, S. 2007, A&A, 465, 41
- Masi, S. et al. 2005, Proc. of the Intl. School of Physics "Enrico Fermi", Course CLIX, IOS Press, The Netherlands, and SIF Bologna, Italy, p.359
- Matthews, W.G. & Brighenti, F. 2007, preprint arXiv:astro-ph/0701712v1
- McNamara, B. R. et al. 2000, AAS, 32.13211
- McNamara, B.R. & Nulsen, P.E.J. 2007, arXiv:0709.2152
- Perez-Torres et al. 2008, arXiv:0812.3598
- Perkins, J.S. et al. 2006, ApJ, 644, 148
- Pfrommer, C., 2008, MNRAS, 385, 1242
- Pfrommer, C. et al. 2006, arXiv:astro-ph/0611085
- Profumo, S. 2008, arXiv:0801.0740
- Ryu, D. et al. 2003, arXiv:astro-ph/0305164
- Sanders, J.S., Fabian, A.C. & Dunn, R.J.H., 2005, MNRAS, 360, 133
- Sanders, J.C. & Fabian, A.C. 2007, arXiv:0705.2712
- Sarazin, C.L. 2001, arXiv:astro-ph/0105418
- Sigl, G. et al. arXiv:astro-ph/0409098

- Shaposhnikov, M. 2007, arXiv:astro-ph/0703673
- Springel, V. et al. 2005, arXiv:astro-ph/0504097
- Takahashi, T. et al. 2004, New AR, 48, 269